

Photoinduced Quasi-2D to 3D Phase Transformation in Hybrid Halide Perovskite Nanoplatelets

Mrinmoy Roy, Vikram, Bhawna, Aftab Alam, M. Aslam*

Indian Institute of Technology Bombay, Powai, Mumbai, India 400076

Synthesis of Hybrid Perovskite Nanoplatelets

1-octadecene (ODE, Sigma-Aldrich, 90%), oleic acid (OA, Sigma-Aldrich, 90%), oleylamine (OAm, technical grade, Sigma-Aldrich 70%), methylamine (CH_3NH_2 , Sigma-Aldrich, 2M solution in tetrahydrofuran, THF), lead bromide (PbBr_2 , Sigma-Aldrich, 98%) and toluene (Merck, HPLC grade) was used as received, without any further purification.

In a typical experiment, 0.18 mmol, i.e., 69 mg of PbBr_2 was loaded into a 100 mL 3-neck round-bottom flask and heated to 120°C in ODE. 0.6 ml OA with 0.5 ml OAm were added into the reaction mixture at 120°C under N_2 flow. The mixture was kept under this condition for an hour. After complete solubilization of PbBr_2 salt, the temperature was decreased to 60°C . After that, 0.17 ml of 2M methylamine solution in THF with 0.7 ml of OA were injected rapidly, which causes instantaneous perovskite NPLs formation. Perovskite NPLs were separated by centrifugation at 8000 rpm for 10 min. The supernatant was discarded and samples were stored in a desiccator.

Computational details for Calculation of various optical properties

Ab-initio calculations were performed to obtain the ground state energy and the dielectric constants of MAPbBr_3 NPLs using Density Functional Theory (DFT)¹ as implemented in Vienna Ab initio Simulation Package (VASP).²⁻⁴ Projector Augmented Wave (PAW)⁵ pseudopotentials with semi-local PBE exchange-correlation functional⁶ were used in order to take the contributions of the core electrons in addition to the valence electrons, under the frozen core approximation. Tetrahedron method with Blöchl corrections⁷ was used for accurate estimation of the bulk ground state energies. A kinetic energy cut off of 500 eV was used to describe the plane waves. A complete cell relaxation was done using conjugate gradient algorithm with a force accuracy criterion of $0.01 \text{ eV}/\text{\AA}$ and an automated Γ centred K-point mesh of $6\times 6\times 6$ in the Brillouin zone. The self-consistent-field (scf) calculations were done within an energy convergence of 10^{-6} eV using a $10\times 10\times 10$ uniform K-point mesh. MAPbBr_3 was simulated in the experimentally stable cubic 12 atom unit cell (space group Pm-3m, #221). The frequency dependent dielectric function was obtained within the independent particle approximation as implemented in VASP. Carrier effective masses at the band edges were calculated using the Effective Mass Calculator code (EMC).⁸ In order to simulate the 2D layered structures of MAPbBr_3 , 2, 3, 4 and 5 layered structures were modelled along the (001) direction. A vacuum of 15 \AA was used to avoid the interaction between the periodic images. Heyd-Scuseria-Ernzerhof (HSE) exchange correlation functional (HSE06) with the van-der-

waals interaction of DFT-D3 was used to make a more accurate bandgap estimate of the surface slabs.

Confinement in Hybrid Layered Perovskites: 2D to Quasi-2D to 3D

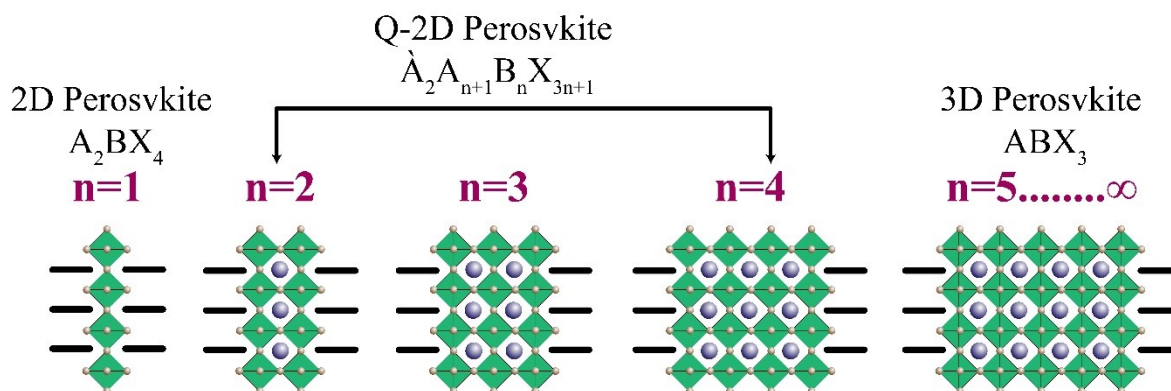


Figure S1 Schematic diagram of 2D, Q-2D and 3D perovskite structure. Complete 2D and 3D perovskite have a chemical formula of A_2BX_4 and ABX_3 , whereas the general chemical formula for quasi-2D perovskite is $\text{A}_2\text{A}_{n+1}\text{B}_n\text{X}_{3n+1}$, where “n” is the thickness of the perovskite slab. For a complete 2D perovskite, the value of n is 1, and for a complete 3D perovskite, the value of n is greater than 5, and in-between from $n = 2$ to 4, the system is referred as the quasi-2D perovskite.

Ruddlesden–Popper phase is a type of perovskite where two-dimensional perovskite-like slabs are interleaved with different cations.^{9–11} The general formula of Ruddlesden–Popper phase is $\text{A}_{n+1}\text{Pb}_n\text{Br}_{3n+1}$ for a single cationic system; which can be represented as $\text{A}_2\text{A}_{n+1}\text{Pb}_n\text{Br}_{3n+1}$ for double cationic compound, where A is a small size cation which can be placed in between the octahedra like MA (CH_3NH_3^+), Cs^+ whereas, A is a long chain organic alkylammonium cation and ‘n’ is the thickness of the perovskite slab, i.e., the number of continuous octahedra which are stacked together in the perovskite structure. A continuous array of $[\text{PbX}_4]^{2-}$ octahedra turns Ruddlesden–Popper structure into a 3D perovskite structure. So, for a complete 3D perovskite structure, n tends to infinity (∞) and for a complete 2D perovskite, $n=1$. In between $n = 2$, to 4, they are known as quasi-2D perovskites (Figure S1).^{12, 13} Quasi-2D perovskites are a natural quantum well system where excitons are confined between the perovskite octahedra layer $[\text{PbX}_6]^{4-}$, known as the well-layer. This well-layer is sandwiched between the barrier layer formed by the long-chain organic alkylammonium cations. Due to this well layer, excitons in this structure behave as an ideal 2D system. It is also found that exciton binding energy continuously increases as the thickness of the perovskite decreases.¹⁴ The thickness of the octahedral layers is of the order of the excitonic Bohr radius of the

perovskite, which makes these varying (2-4) layer-thickness perovskite system a natural quantum-confined system. Two and three-layered thick quasi-2D perovskites belong to the strong confinement regime. Four-layer thick quasi-2D perovskite belongs to the weak confinement regime, and five and more layers of thick perovskites behave like bulk perovskite.

15

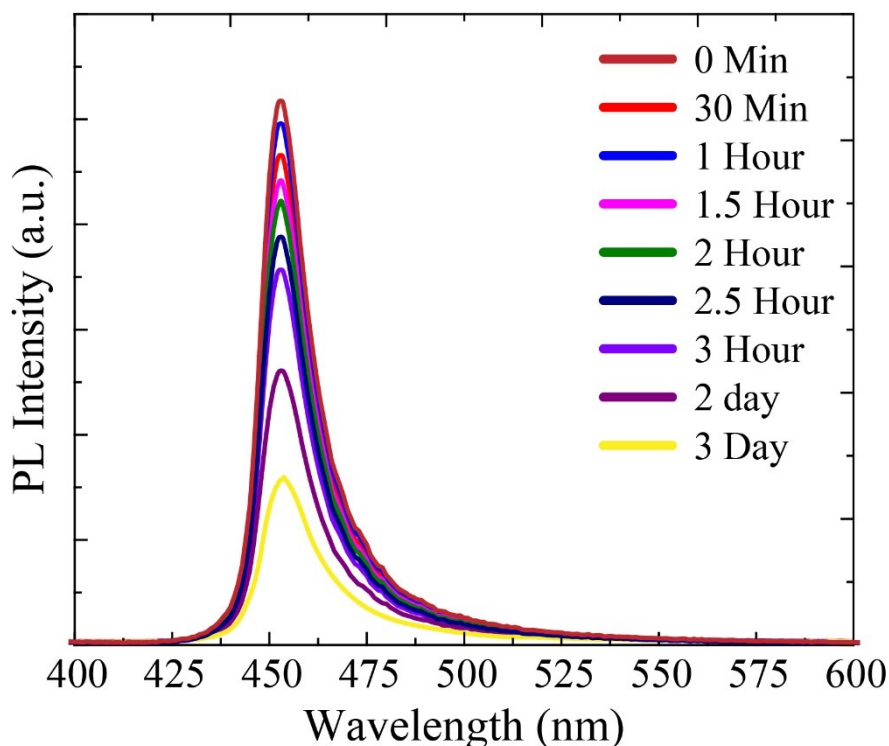


Figure S2 Shows time dependent PL emission of two-layer thick MAPbBr₃ perovskite NPLs which out photon irradiation, which confirms that no phase change over the time as no change is observed in the emission peak position.

Reference

1. P. Hohenberg and W. Kohn, *Physical Review*, 1964, **136**, B864-B871.
2. G. Kresse and J. Furthmüller, *Physical Review B*, 1996, **54**, 11169-11186.
3. G. Kresse and J. Furthmüller, *Computational Materials Science*, 1996, **6**, 15-50.
4. G. Kresse and J. Hafner, *Physical Review B*, 1993, **47**, 558-561.
5. P. E. Blöchl, *Physical Review B*, 1994, **50**, 17953-17979.
6. J. P. Perdew, K. Burke and M. Ernzerhof, *Physical Review Letters*, 1996, **77**, 3865-3868.
7. P. E. Blöchl, O. Jepsen and O. K. Andersen, *Physical Review B*, 1994, **49**, 16223-16233.

8. A. Fonari and C. J. c. b. f. u. h. g. c. a. Sutton, nd, 2012.
9. S. Ruddlesden and P. J. A. C. Popper, 1958, **11**, 54-55.
10. X. Gao, X. Zhang, W. Yin, H. Wang, Y. Hu, Q. Zhang, Z. Shi, V. L. Colvin, W. W. Yu and Y. Zhang, *Advanced Science*, 2019, **6**, 1900941.
11. Y.-H. Chang, J.-C. Lin, Y.-C. Chen, T.-R. Kuo and D.-Y. Wang, *Nanoscale Research Letters*, 2018, **13**, 247.
12. I. Levchuk, P. Herre, M. Brandl, A. Osvet, R. Hock, W. Peukert, P. Schweizer, E. Spiecker, M. Batentschuk and C. J. Brabec, *Chemical Communications*, 2017, **53**, 244-247.
13. Y. Tong, F. Ehrat, W. Vanderlinden, C. Cardenas-Daw, J. K. Stolarczyk, L. Polavarapu and A. S. Urban, *ACS Nano*, 2016, **10**, 10936-10944.
14. K. Tanaka and T. Kondo, *Science and Technology of Advanced Materials*, 2003, **4**, 599-604.
15. L. Liang and P. Gao, *Advanced Science*, 2018, **5**, 1700331.